RESEARCH ARTICLE

Explosive transitions to synchronization in networks of frequency dipoles

Liuhua Zhu[1,2,3]*, **Shu Zhu**[1]

1 School of Physics and Telecommunication Engineering, Yulin Normal University, Yulin, Guangxi, China,
2 Guangxi Colleges and Universities Key Laboratory of Complex System Optimization and Big Data
Processing, Yulin Normal University, Yulin, Guangxi, China, **3** Optoelectronic Information Research Center,
Yulin Normal University, Yulin, Guangxi, China

☯ These authors contributed equally to this work.
* lhzhu@ylu.edu.cn

Abstract

We reveal that an introduction of frequency-weighted inter-layer coupling term in networks
of frequency dipoles can induce explosive synchronization transitions. The reason for explosive synchronization is that the oscillators with synchronization superiority are moderately
suppressed. The findings show that a super-linear correlation induces explosive synchronization in networks of frequency dipoles, while a linear or sub-linear correlation excites chimera-like states. Clearly, the synchronization transition mode of networks of frequency
dipoles is controlled by the power-law exponent. In addition, by means of the mean-field
approximation, we obtain the critical values of the coupling strength within and between layers in two limit cases. The results of theoretical analysis are in good agreement with those of
numerical simulation. Compared with the previous models, the model proposed in this
paper retains the topological structure of network and the intrinsic properties of oscillators,
so it is easy to realize pinning control.

Introduction

Synchronization is widely distributed in human society and natural environment. Synchronization in human society requires a unified command driven by external factors. For instance,
when the monitor suddenly calls "stand up" in class, everyone stands up in unison, which is
the synchronization mechanism under a unified command. However, the formation of synchronization in natural environment mainly depends on the cohesion of the system itself. In
order to grasp the synchronous behaviors of complex systems, the synchronization dynamics
of coupled phase oscillators has been widely studied in recent years [1–4]. Among the collective phenomena observed in these systems, the chimera states of coupled phase oscillators have
aroused great interest of researchers [5–13]. The chimera state here refers to a transient state
in the process of synchronization transition, in which some oscillators are locked and the
remaining ones are in the drift state, that is, a coexistence state of synchronization and
drifting.

In the past, researchers always thought that the synchronization in networks of coupled
oscillators was a continuous and gradual phase transition process. This one-sided opinion was

not ended until an explosive synchronization was found [14]. The so-called explosive synchronization means that the mode of synchronization transition is sudden without any omen. In the relation curve of order parameter versus coupling strength, the order parameter will jump sharply when the coupling strength increases to the critical value of the system. Meanwhile, the system transits abruptly from synchronization to incoherence state as the coupling strength is decreased, and the forward and backward continuations do not overlap, which results in a hysteresis loop [15–24].

In the field of electro-magnetism, how to analyze the polarization phenomenon of dielectric, the first thing is to discretize the dielectric into a system composed of multiple electric dipoles. In medical research, some dipole source models that produce scalp potential are established to speculate the source of electrical activity in the brain [25]. In industrial automation devices, when the ferromagnetic target is far enough from the sensor, it can be regarded as a magnetic dipole [26]. Inspired by these ideas, we try to discretize a complex system into a network composed of frequency dipoles. A double-layer network is considered because only one single-layer network is not enough to place multiple pairs of frequency dipoles. In this way, we can use the tool of complex network to study the dynamical behavior of complex systems [27].

Recently, the synchronization dynamics of multiplex networks has been deeply and carefully studied by employing different methodologies, for instance, phase-shift [28], adaptive inter-layer coupling [29], and inter-layer Hebbian plasticity [30]. As for the choice of coupled oscillators, the Kuramoto oscillator is the most mature and widely used tool in the research field of synchronization theory [31, 32], so it has also become our first choice. We use a double-layer network composed of two globally connected layers as the substrates, in which the upper and lower oscillators form frequency dipoles.

The follow-up parts of this paper are organized as follows. First of all, some basic notions on the frequency dipoles are introduced. In the next place, we give the main results of numerical simulations. Once again, the theoretical analysis and numerical simulation are carried out for the critical values of coupling strength within and between layers in two limit cases. Finally, we summarize our main findings and discuss open problems.

Materials and methods

Description of network model

We consider a two-layer network, in which each layer is composed of N globally connected nodes. In order to realize the connection between the two layers, N edges are added between the nodes with the same label in the upper and lower layers. After this step, a two-layer network similar to the pavilion structure is completed. The number of edges of the whole network is N^2.

To explore the dynamics behavior of this network, each node in the network is embedded with a variant Kuramoto oscillator. The natural frequency of the ith oscillator in the upper layer is set to $\omega_i^u = -1 + 2(i-1)/(N-1)$. The value of ω_i^l in the lower layer is set to $\omega_i^l = -\omega_i^u$, so a pair of frequency dipoles are formed. Here u and l are identifiers of the upper and lower layers, respectively. The dynamics of the ith oscillator in the network is governed by the following equations,

$$\frac{d\phi_i^u}{dt} = \omega_i^u + \frac{\mu}{N}\sum_{j=1}^{N} sin(\phi_j^u - \phi_i^u) + \lambda|\omega_i^u|^\beta sin(\phi_i^l - \phi_i^u),$$

$$\frac{d\phi_i^l}{dt} = \omega_i^l + \frac{\mu}{N}\sum_{j=1}^{N} sin(\phi_j^l - \phi_i^l) + \lambda|\omega_i^l|^\beta sin(\phi_i^u - \phi_i^l),$$

(1)

where $i = 1, 2, 3, \ldots, N$. The parameter ϕ_i is the instantaneous phase of the ith oscillator. The initial phase of each oscillator is randomly assigned within the range $[-\pi, \pi]$. The nonnegative parameter μ represents the intra-layer coupling strength, whereas the inter-layer coupling strength is denoted with λ.

Three types of positive correlations, i.e., $\beta = 1$, $0 < \beta < 1$ and $\beta > 1$ are considered in this paper, which are also known as linear, sub-linear, and super-linear correlations, respectively. For better comparison, we supplement the case of $\beta = 0$, which corresponds to the homogeneous coupling.

In this paper, the size of each layer is set to $N = 200$ for numerical simulations, unless otherwise specified, because we find that the results described below do not change significantly for larger network sizes. The number of connected edges of each oscillator in these networks is constant, i.e., $k = 200$.

Results

In this part, we reveal the detailed characteristics of frequency synchronization of coupled oscillators. The commonly used method is to introduce the effective frequency, which is defined as follows [14],

$$\Omega_i^{u(l)} = \frac{1}{T} \int_{t_0}^{t_0+T} \dot{\phi_i}^{u(l)}(\tau)d\tau. \tag{2}$$

where t_0 is the relaxation time and T is the length of time used to obtain the average.

Emergence of chimera-like state

Fig 1a and 1b show the snapshots of instantaneous phases and effective frequencies of all oscillators in the upper layer under the case of homogeneous coupling, respectively. The effective frequencies of the oscillators in the central region of the frequency spectrum tend to be the same, but the effective frequencies of the oscillators at both ends of the spectrum fluctuate greatly, which means that there is a chimera-like state. It is worth noting that the phenomenon is not a chimera state in the real sense. In fact, the chimera state is a unique synchronization phenomenon in a system with identical oscillators, whereas these oscillators in this paper are heterogeneous. Therefore, the phenomenon appearing in Fig 1b is called a chimera-like state.

Fig 2a and 2b show that for the linear correlation, the system also induces a chimera-like state. For the homogeneous coupling and the linear correlation, the processes of phase locking and frequency synchronization of coupled oscillators are similar, that is, the central region is synchronized first, and then extends to both ends. It can be inferred that for the sub-linear correlation, the synchronization transition of the system should be gradual rather than abrupt.
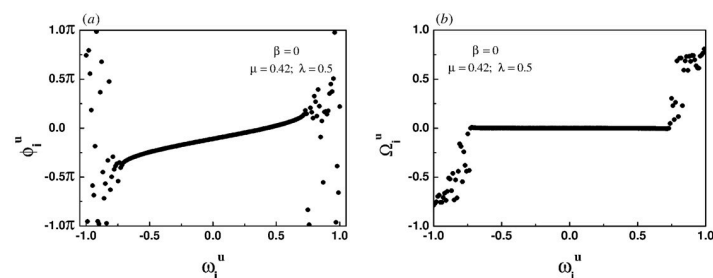
Fig 1. Snapshots of the instantaneous phases (left panel) and the effective frequencies (right panel) for the homogeneous coupling when the intra-layer and inter-layer coupling strength are set to 0.42 and 0.5, respectively.
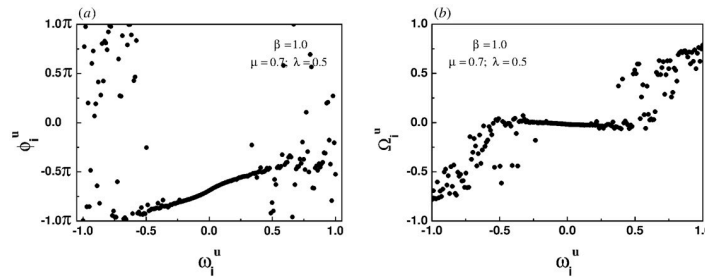
Fig 2. Snapshots of the instantaneous phases (left panel) and the effective frequencies (right panel) for the linear correlation when the intra-layer and inter-layer coupling strength are set to 0.7 and 0.5, respectively.

In order to characterize the coherence degree of the coupled oscillators in each layer, two separate phase order parameters are considered [33],

$$R^{u(l)} e^{i\psi^{u(l)}} = \frac{1}{N} \sum_{j=1}^{N} e^{i\phi_j^{u(l)}} \tag{3}$$

where $R^{u(l)} \epsilon [0, 1]$ is a measure of the coherence of coupled oscillators in the upper (lower) layer. The greater its value, the higher the coherence. The parameter $\psi^{u(l)}$ is the average phase of coupled oscillators in the upper (lower) layer.

In the following numerical simulations, Eq 1 is integrated by the fourth-order Runge-Kutta method with time step 0.01. Excluding the randomness of initial phases, the network parameters of the upper and lower layers are exactly the same. In order to avoid repetition, the evolution law of order parameter of the lower layer is omitted.

Fig 3 shows that for the sub-linear correlation, a continuous phase transition does occur in the system, which confirms our above inference. However, due to the strong coupling between layers, the system cannot return to the original state after desynchronization. The smaller the value of β, the worse the desynchronization performance, as shown in Fig 3a.

Emergence of explosive synchronization

Fig 4a and 4b show the snapshots of instantaneous phases and effective frequencies of all oscillators in the upper layer under the case of linear correlation, respectively. As shown in Fig 4b, the effective frequencies of the oscillators located in the central region of the frequency
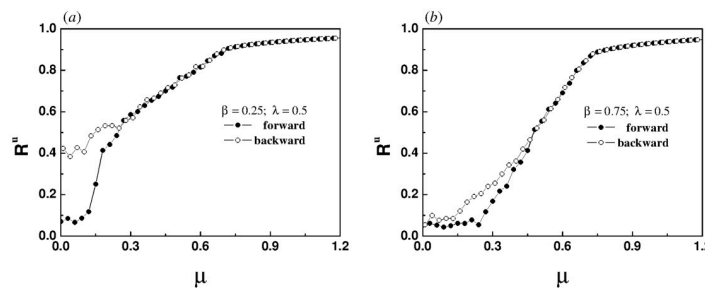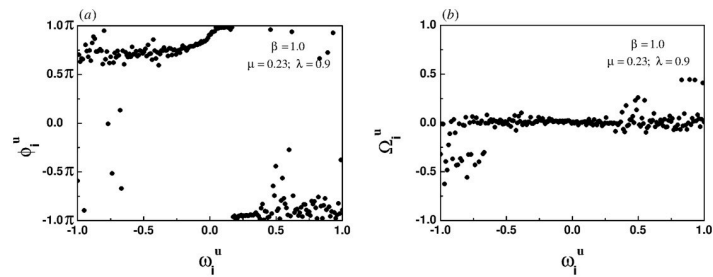

Fig 3. The evolution of order parameter of the upper layer with the increase of intra-layer coupling strength for different values of β, (a) $\beta = 0.25$, (b) $\beta = 0.75$. The inter-layer coupling strength λ is set to 0.5. Every data point in the two panels is the average of 2000 time steps after discarding the initial 2000 time steps.

Fig 4. Snapshots of the instantaneous phases (left panel) and the effective frequencies (right panel) for the linear correlation when the intra-layer and inter-layer coupling strength are set to 0.23 and 0.9, respectively.

spectrum are convergent, while the effective frequencies of the oscillators located at both ends of the spectrum are divergent, indicating the emergence of a chimera-like state.

Fig 5a and 5b show that for the super-linear correlation, the system also induces a chimera-like state. However, the process of phase locking and frequency synchronization first occurs at both ends, and then gradually spreads to the middle, which is just opposite to Fig 4.

For the case of $\beta = 1$, the frequency synchronization of coupled oscillators starts in the middle of the spectrum, but for $\beta = 2$, the frequency synchronization first occurs at both ends of the spectrum. We speculate that if β takes a value between 1 and 2, the oscillators in the system will not be able to determine the location where synchronization occurs first. Therefore, the oscillators in the system reach a consensus, either out of synchronization or collective synchronization, which leads to the emergence of explosive synchronization.

To verify this speculation, both synchronization and desynchronization diagrams are plotted for two different values of β, as shown in Fig 6. For the super-linear correlation, the system does induce an explosive synchronization. However, due to the influence of inter-layer coupling, the system can not return to the original state after desynchronization.

For the super-linear correlation, why does the network induce an explosive synchronization? Our theoretical explanation is as follows. The frequencies of the oscillators who located in the central region of the spectrum of natural frequency are close to the frequency of ensemble equilibrium state, so they are most likely to evolve into condensation nuclei of network synchronization, that is, to achieve synchronization first. However, the oscillators at both ends of the spectrum enjoy greater relative inter-layer coupling strength. Here, the relative inter-layer coupling strength refers to the ratio of the absolute inter-layer coupling strength to the positive natural frequency of the frequency dipoles, i.e., $\lambda_r = \lambda |\omega_i^u|^\beta / |\omega_i^u| = \lambda |\omega_i^u|^{1-\beta}$. Due to
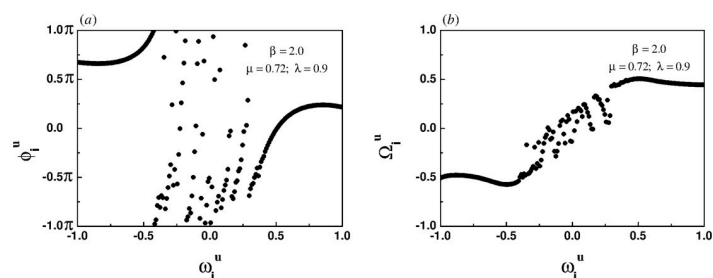
Fig 5. Snapshots of the instantaneous phases (left panel) and the effective frequencies (right panel) for the super-linear correlation when the intra-layer and inter-layer coupling strength are set to 0.72 and 0.9, respectively.
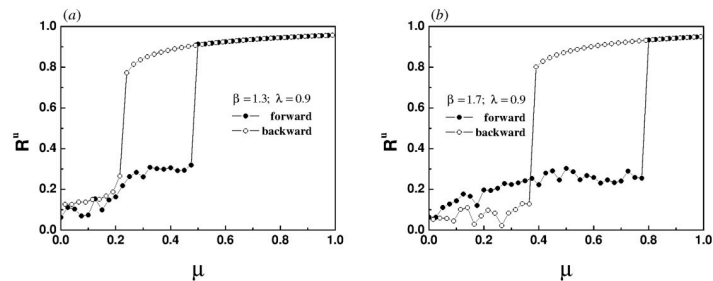
Fig 6. The evolution of order parameter of the upper layer with the increase of intra-layer coupling strength when the inter-layer coupling strength λ is set to 0.9. Both of them correspond to the super-linear correlations, (a) $\beta = 1.3$, (b) $\beta = 1.7$. Every data point in the two panels is the average of 2000 time steps after discarding the initial 2000 time steps.

the difference of advantages, each oscillator in the network has equal opportunity to evolve into the first synchronous condensation center. As long as their advantages are balanced, an explosive synchronization will be ignited.

Next, we keep the intra-layer coupling strength unchanged and study the synchronization transition characteristics of coupled oscillators by increasing the inter-layer coupling strength. The same law is found that the second-order phase transition occurs in the sub-linear coupled system, as shown in Fig 7a. It is easy to see that there is a hysteresis loop in the super-linear coupled system, indicating the emergence of explosive synchronization, as shown in Fig 7b. It is worth noting that the desynchronization effect is the most thorough in this system.

Now we systematically study the influence of power-law exponents on the synchronization transition of coupled oscillators. In Fig 8, the order parameter of the upper layer is described by chromaticity in the $\lambda - \mu$ parameter plane for different power-law exponents. It is generally realized that with the increase of the coupling strength within and between layers, the oscillators in the network tend to be synchronized. The simulation results are consistent with our intuition. For the homogeneous coupling, sub-linear correlation and linear correlation, the boundary lines between different degrees of synchronization is clear and recognizable, as shown in Fig 8a–8c. Nevertheless, for the super-linear correlation the boundary lines between different degrees of synchronization are intertwined and even distorted in certain areas as shown in Fig 8d, which may be the internal cause of the emergence of explosive synchronization.

Let us now investigate the influence of system size on the hysteresis loop width. Fig 9a shows the forward and backward continuous diagrams of upper layers of different sizes. It is
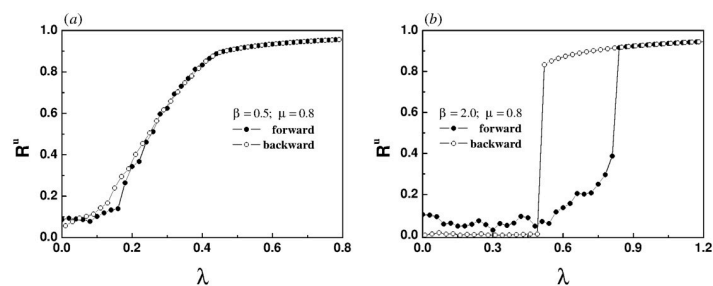
Fig 7. The evolution of order parameter of the upper layer with the increase of inter-layer coupling strength for different values of β, (a) $\beta = 0.5$, (b) $\beta = 2.0$. The intra-layer coupling strength μ is set to 0.8. Every data point in the two panels is the average of 2000 time steps after discarding the initial 2000 time steps.
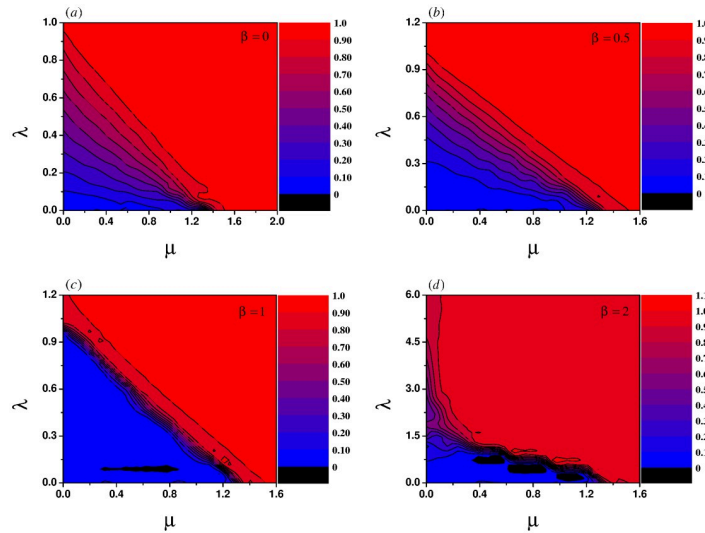
Fig 8. Order parameter of the upper layer is described by chromaticity in the $\lambda - \mu$ parameter plane. The chromaticity ranges from 0 (black) to 1 (red). The greater its value, the higher the degree of phase coherence. The values of β in each panel are (a) $\beta = 0$, (b) $\beta = 0.5$, (c) $\beta = 1$, (d) $\beta = 2$, respectively.

found that the width of the hysteresis loop increases with the size of the system until it reaches saturation. However, there is an interesting phenomenon in the process of backward transition. As shown in Fig 9a, the critical point of the backward continuation in the model is robust, which does not change with the increase of system size [14, 16]. For each size, there is a pair of corresponding forward and backward transition points μ_f and μ_b, with $d = \mu_f - \mu_b$. Fig 9b reports the corresponding dependence of $< d >$ on N for twenty realizations. The simulation results show that when the size of the upper layer increases to $N = 700$ (the size of the lower layer changes synchronously) the width of the hysteresis loop tends to be saturated, which also indicates that the characteristics of explosive synchronization in the system have not changed. Fig 9 verifies that an increase in system size does not change the type of synchronization transition.

Theoretical analysis

In this section, we give the critical values of intra-layer and inter-layer coupling strength in two limit cases from the perspective of theoretical analysis. Considering the case of $\lambda = 0$, the
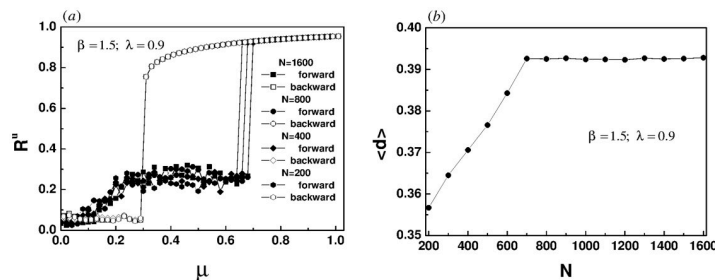
Fig 9. (a) Synchronization and desynchronization diagrams of upper layers with different sizes. (b) Dependence of hysteresis loop width on network size. Other parameters are set to $\beta = 1.5$ and $\lambda = 0.9$.

bilayer network is split into two incoherent globally connected networks. The critical value of intra-layer coupling strength is obtained [33],

$$\mu_c = \frac{2}{\pi g(0)} = \frac{4}{\pi} \approx 1.27 \tag{4}$$

where $g(\cdot)$ is a probability distribution function. The four panels in Fig 8 show that the position where the blue area disappears on the horizontal axis occurs at about $\mu = 1.3$. Obviously, our theoretical analysis is consistent with the numerical simulation.

When the connection between the two layers is restored, the average coupling strength of each edge is given by,

$$\bar{\lambda} = \frac{1}{N} \sum_{i=1}^{N} \lambda |\omega_i^{u(l)}|^\beta \approx \frac{1}{N} \frac{2 \int_0^1 \lambda \omega^\beta d\omega}{2/N} = \frac{\lambda}{1+\beta} \tag{5}$$

Eq 5 shows when the values of λ and μ remain unchanged, the increased β weakens the synchronization ability of the network. When the value of β increases, it causes the intersections between the boundary lines with different degrees of synchronization and the longitudinal axis to move upward, as shown in Fig 8.

The left and right sides of Eq 3 are multiplied by a factor $e^{-i\phi_i^{u(l)}}$ and substituted into Eq 1. Note that the first i in the factor is an imaginary unit and the second i is the label of the oscillator. Eq 1 can be rewritten as,

$$
\begin{aligned}
\frac{d\phi_i^u}{dt} &= \omega_i^u + \mu R^u sin(\psi^u - \phi_i^u) + \lambda |\omega_i^u|^\beta sin(\phi_i^l - \phi_i^u), \\
\frac{d\phi_i^l}{dt} &= \omega_i^l + \mu R^l sin(\psi^l - \phi_i^l) + \lambda |\omega_i^l|^\beta sin(\phi_i^u - \phi_i^l),
\end{aligned}
\tag{6}
$$

We mainly discuss the influence of inter-layer coupling on synchronization transition of the network in the case of $\mu \to 0$. Except that the distribution of initial phases is slightly different due to randomness, the other parameters of the upper and lower layers are exactly the same. Therefore, these equations hold after the system reaches a stable synchronous state, i.e., $d\phi_i^u/dt = d\phi_i^l/dt$, $R^u = R^l$ and $\psi^u = \psi^l$. Ignoring the intra-coupling term, Eq 6 for a pair of frequency dipoles becomes,

$$
\begin{aligned}
0 &= \omega_i^u + \lambda |\omega_i^u|^\beta sin(\phi_i^l - \phi_i^u), \\
0 &= \omega_i^l + \lambda |\omega_i^l|^\beta sin(\phi_i^u - \phi_i^l),
\end{aligned}
\tag{7}
$$

Thus the relationship between phase difference and the inter-coupling strength can be rewritten as,

$$
\begin{aligned}
\lambda &= -|\omega_i^u|^{1-\beta}/sin(\phi_i^l - \phi_i^u) & \omega_i^u > 0, \\
\lambda &= |\omega_i^l|^{1-\beta}/sin(\phi_i^u - \phi_i^l) & \omega_i^l < 0,
\end{aligned}
\tag{8}
$$

In view of the boundedness of sinusoidal function, it is easy to obtain the critical value of λ,

$$\lambda_c = \left|\omega_i^{u(l)}\right|^{1-\beta} \tag{9}$$

Fig 10a shows the dependence of R^u on λ in the case of $\beta = 1$. It is easy to see that the order parameter undergoes a continuous transition, where the incoherent state with $R^u \approx 0$ is destabilized via a supercritical Hopf bifurcation at $\lambda = 1.0$ [34]. It is in perfect agreement with the
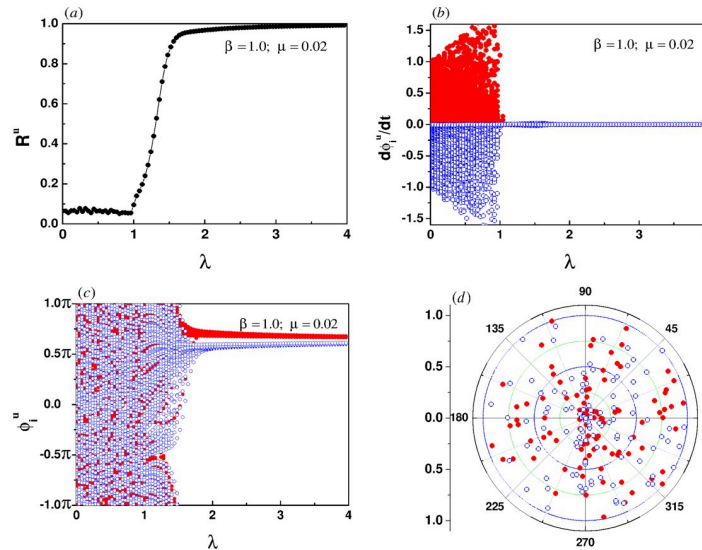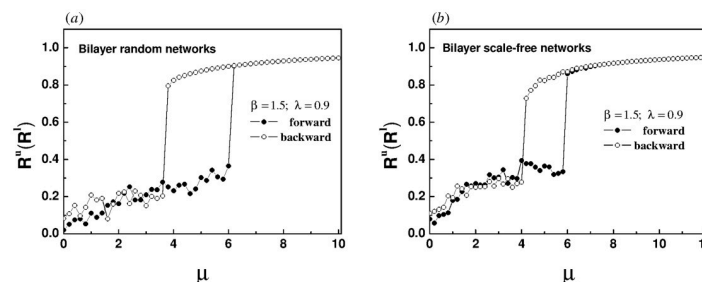
Fig 10. (a) The evolution of order parameter of the upper layer for the linear correlation. (b) and (c) show the evolutions of instantaneous frequencies and phases of the oscillators, respectively. (d) is the snapshot of instantaneous phases at $\lambda = 1.0$. The intra-layer coupling strength is set to 0.02. The red solid circles represent the oscillators with positive natural frequencies, while the oscillators with negative natural frequencies are described by blue hollow circles.

https://doi.org/10.1371/journal.pone.0274807.g010

theoretical result of Eq 9. The simulation results show that in this case the instantaneous frequencies of all oscillators have been synchronized as shown in Fig 10b, and the phase locking has just started, as shown in Fig 10c. Fig 10d exhibits the detailed characteristics of phase distribution of the oscillators. The oscillators are almost evenly scattered on the circular plane, the phases are unlocked, and the order parameter tends to zero in the macro view. The process of phase locking continues until the phases of all oscillators are locked when $\lambda \approx 1.8$, as shown in Fig 10c.

Discussion

Furthermore, for the super-linear correlation we reconstructed the bilayer network, in which both the upper and lower layers of Fig 11a are random networks, both the upper and lower

Fig 11. The panels show the evolution of order parameter of the upper layer with the increase of intra-layer coupling strength for different network topologies, (a) both the upper and lower layers are random networks, (b) both the upper and lower layers are scale-free networks. The inter-layer coupling strength λ is set to 0.9. The natural frequency of each oscillator in the upper layer is randomly selected in the interval [-1, 1], and the natural frequency of oscillators with the same label in the lower layer changes synchronously. Because the upper and lower networks belong to the same type, the evolution of order parameters is almost the same. In order to avoid repetition, the evolution law of order parameter of the lower layer is omitted.

https://doi.org/10.1371/journal.pone.0274807.g011
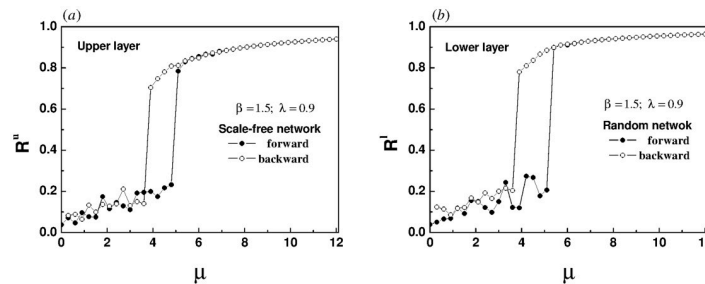
Fig 12. The panels show the evolution of order parameters of the upper (a) and lower (b) layers with the increase of intra-layer coupling strength for a bilayer network composed of a scale-free network in the upper layer and a random network in the lower layer. The inter-layer coupling strength λ is set to 0.9. The natural frequency of each oscillator in the upper layer is randomly selected in the interval [-1, 1], and the natural frequency of oscillators with the same label in the lower layer changes synchronously.

layers of Fig 11b are scale-free networks, the upper layer of Fig 12 is a scale-free network, and the lower layer is a random network. For all subsequent simulations, each layer of the network has 200 nodes and 2000 edges. The natural frequency of each oscillator in the upper layer is no longer forcibly specified, but is randomly selected within the interval [-1, 1]. The essence of a pair of frequency dipoles composed of oscillators with the same label in the upper and lower layers continues to be retained. The initial phase of each oscillator is randomly assigned within the range $[-\pi, \pi]$. Every data point in Figs 11 and 12 is the average of 2000 time steps, after discarding the initial 2000 time steps.

Obviously, hysteresis loops appear in the four panels of Figs 11 and 12, indicating that an explosive synchronization has emerged in both the upper and lower layers. Whether the upper and lower layers are homogeneous or heterogeneous, the super-linear correlation will induce an explosive synchronization.
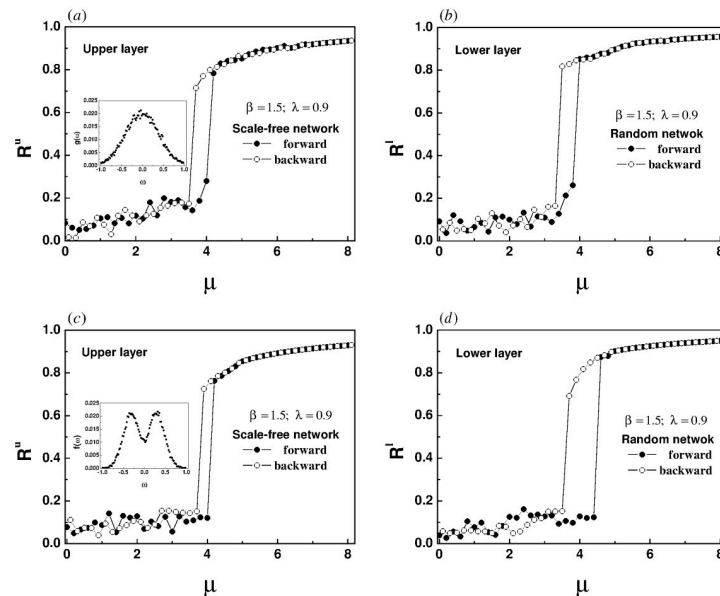
Next, we use two different natural frequency distributions and maintain the same network topology as in Fig 12. Here two typical symmetric distributions, unimodal and bimodal Gaussian distributions, are considered. Fig 13 plots the dependence of $R^u(R^l)$ and λ for two different natural frequency distributions. In Fig 13a and 13b, we replace the random uniform distribution by a unimodal Gaussian distribution. The probability density function $g(\omega) = \frac{1}{\sqrt{2\pi}\sigma} e^{\frac{-(\omega-\omega_0)^2}{2\sigma^2}}$ satisfies the symmetry condition, in which $\omega_0 = 0$ and $\sigma^2 = 0.16$, as shown in the small inset of Fig 13a. The bimodal Gaussian distribution follows $f(\omega) = A(\omega^2 + B^2)e^{\frac{-(\omega-\omega_0)^2}{2\sigma^2}}$, with $A = 20.3108$, $B = 0.1667$, $\omega_0 = 0$ and $\sigma^2 = 0.0566$, as shown in the small inset of Fig 13c. Fig 13 reproduces the same scene as Fig 12. For these two different symmetrical frequency distributions, explosive synchronizations are also activated, independent of network topology. In addition, two kinds of asymmetric frequency distributions, power-law distribution and Rayleigh distribution are tested, which failed to trigger an explosive synchronization. The corresponding synchronization and desynchronization diagrams are not given in this paper. We conclude that only when the natural frequencies of the oscillators satisfy the symmetric distribution, the super-linear correlation can excite an explosive synchronization.

Conclusion

In this paper, inspired by the idea of the electric dipoles and frequency weighting, the coupling-frequency correlations are introduced into a symmetric two-layer network. The effects

Fig 13. Synchronization and desynchronization transition diagrams of each layer at different natural frequency distributions. The topology of the network is exactly the same as Fig 12. We replace the random uniform distribution by two symmetric frequency distributions. The small inset in Fig 13a is a unimodal Gaussian distribution, in which the parameters are set to $\omega_0 = 0$ and $\sigma^2 = 0.16$. The small inset in Fig 13c is a bimodal Gaussian distribution, in which the parameters are set to $A = 20.3108$, $B = 0.1667$, $\omega_0 = 0$ and $\sigma^2 = 0.0566$.

https://doi.org/10.1371/journal.pone.0274807.g013

of three typical correlations on synchronization transition of coupled oscillators are studied in detail.

For the sub-linear correlation, the oscillators in the center of the frequency spectrum have two superiorities in the synchronization transition. On the one hand, their natural frequencies are closer to the steady state of the ensemble, which makes them locked first. On the other hand, they obtain greater relative inter-layer coupling, in which the relative inter-layer coupling refers to the ratio of absolute inter-layer coupling to the natural frequency. The two superiorities contribute to the emergence of chimera-like states.

For the linear correlation, there is no difference in relative inter-layer coupling strength. Naturally, the oscillators whose natural frequencies are closer to the steady state of the ensemble tend to be synchronized first, resulting in chimera-like states.

For the super-linear correlation, the oscillators located at the center of the frequency spectrum have the location advantage, while the oscillators in the ends of frequency spectrum have the superiority of larger relative inter-layer coupling strength. When the two superiorities are well-matched in strength, an explosive synchronization occurs. Therefore, the network of frequency dipoles can be considered as one of the effective models to describe the complex system where chimera-like states and explosive synchronization are pervasive.

Supporting information

S1 Data. Minimal data set. This compressed file covers the data information of all pictures in the manuscript.
(ZIP)

Acknowledgments

We are very grateful to the editors and reviewers for their constructive comments.

Author Contributions

Formal analysis: Liuhua Zhu.

Investigation: Shu Zhu.

Methodology: Liuhua Zhu.

Software: Shu Zhu.

Supervision: Liuhua Zhu.

Visualization: Shu Zhu.

Writing – original draft: Liuhua Zhu.

References

1. Arenas A, Diaz-Guilera A, Kurths J, Moreno Y, Zhou CS. Synchronization in complex networks. Phys. Rep. 2008 Dec; 469(3):93–153. https://doi.org/10.1016/j.physrep.2008.09.002

2. Boccaletti S, Almendral JA, Guan S, Leyva I, Liu Z, Sendina-Nadal I, et al. Explosive transitions in complex networks' structure and dynamics: Percolation and synchronization. Phys. Rep. 2016 Nov; 660 (17):1–94. https://doi.org/10.1016/j.physrep.2016.10.004

3. Millan AP, Torres JJ, Bianconi G. Complex Network Geometry and Frustrated Synchronization. Sci. Rep. 2018 Jul; 8:9910. https://doi.org/10.1038/s41598-018-28236-w PMID: 29967410

4. Ghosh D, Frasca M, Rizzo A, Majhi S, Rakshit S, Alfaro-Bittner K, et al. The synchronized dynamics of time-varying networks. Phys. Rep. 2022 Feb; 949:1–63. https://doi.org/10.1016/j.physrep.2021.10.006

5. Zhu Y, Zheng ZG, Yang JZ. Chimera states on complex networks. Phys. Rev. E 2014 Feb; 89:022914. https://doi.org/10.1103/PhysRevE.89.022914 PMID: 25353552

6. Kundu S, Majhi S, Bera BK, Ghosh D, Lakshmanan M. Chimera states in two-dimensional networks of locally coupled oscillators. Phys. Rev. E 2018 Feb; 97:022201. https://doi.org/10.1103/PhysRevE.97.022201 PMID: 29548198

7. Rode J, Totz JF, Fengler E, Engel H. Chimera States on a Ring of Strongly Coupled Relaxation Oscillators. Front. Appl. Math. Stat. 2019 Jun; 5:31. https://doi.org/10.3389/fams.2019.00031

8. Sawicki J, Ghosh S, Jalan S, Zakharova A. Chimeras in Multiplex Networks: Interplay of Inter- and Intra-Layer Delays. Front. Appl. Math. Stat. 2019 Apr; 5:19. https://doi.org/10.3389/fams.2019.00019

9. Suda Y, Okuda K. Emergence of second coherent regions for breathing chimera states. Phys. Rev. E 2020 Jun; 101:062203. https://doi.org/10.1103/PhysRevE.101.062203 PMID: 32688598

10. Frolov N, Maksimenko V, Majhi S, Rakshit S, Ghosh D, Hramov A. Chimera-like behavior in a heterogeneous Kuramoto model: The interplay between attractive and repulsive coupling. Chaos 2020 Aug; 30:081102. https://doi.org/10.1063/5.0019200 PMID: 32872824

11. Simo GR, Njougouo T, Aristides RP, Louodop P, Tchitnga R, Cerdeira HA. Chimera states in a neuronal network under the action of an electric field. Phys. Rev. E 2021 Jun; 103:062304. https://doi.org/10.1103/PhysRevE.103.062304 PMID: 34271625

12. Rontogiannis A, Provata A. Chimera states in FitzHugh-Nagumo networks with reflecting connectivity. Eur. Phys. J. B 2021 May; 94:97. https://doi.org/10.1140/epjb/s10051-021-00097-9

13. Parastesh F, Jafari S, Azarnoush H, Shahriari Z, Wang Z, Boccaletti S, et al. Chimeras. Phys. Rep. 2021 Mar; 898:1–114. https://doi.org/10.1016/j.physrep.2020.10.003

14. Gomez-Gardenes J, Gomez S, Arenas A, Moreno Y. Explosive Synchronization Transitions in Scale-Free Networks. Phys. Rev. lett. 2011 Mar; 106:128701. https://doi.org/10.1103/PhysRevLett.106.128701 PMID: 21517358

15. Leyva I, Navas A, Sendina-Nadal I, Almendral JA, Buldu JM, Zanin M, et al. Explosive transitions to synchronization in networks of phase oscillators. Sci. Rep. 2013 Feb; 3:01281. https://doi.org/10.1038/srep01281 PMID: 23412391

16. Zhang XY, Hu X, Kurths J, Liu ZH. Explosive synchronization in a general complex network. Phys. Rev. E 2013 Jul; 88:010802. https://doi.org/10.1103/PhysRevE.88.010802

17. Zhang XY, Zou Y, Boccaletti S, Liu ZH. Explosive synchronization as a process of explosive percolation in dynamical phase space. Sci. Rep. 2014 Jun; 4:05200. https://doi.org/10.1038/srep05200 PMID: 24903808

18. Zhang XY, Boccaletti S, Guan SG, Liu ZH. Explosive Synchronization in Adaptive and Multilayer Networks. Phys. Rev. Lett. 2015 Jan; 114:038701. https://doi.org/10.1103/PhysRevLett.114.038701 PMID: 25659026

19. Khanra P, Kundu P, Hens C, Pal P. Explosive synchronization in phase-frustrated multiplex networks. Phys. Rev. E 2018 Nov; 98:052315. https://doi.org/10.1103/PhysRevE.98.052315

20. Soriano-Panos D, Guo Q, Latora V, Gomez-Gardenes J. Explosive transitions induced by interdependent contagion-consensus dynamics in multiplex networks. Phys. Rev. E 2019 Jun; 99:062311. https://doi.org/10.1103/PhysRevE.99.062311 PMID: 31330755

21. Jalan S, Kumar A, Leyva I. Explosive synchronization in frequency displaced multiplex networks. Chaos 2019 Apr; 29:041102. https://doi.org/10.1063/1.5092226 PMID: 31042936

22. Jalan S, Kachhvah AD, Jeong H. Explosive synchronization in multilayer dynamically dissimilar networks. J COMPUT SCI-NETH 2020 Oct; 46:101177. https://doi.org/10.1016/j.jocs.2020.101177

23. Sharma A. Explosive synchronization through attractive-repulsive coupling. Chaos, Solitons and Fractals 2021 Apr; 145:110815. https://doi.org/10.1016/j.chaos.2021.110815

24. Roy M, Poria S, Hens C. Assortativity-induced explosive synchronization in a complex neuronal network. Phys. Rev. E 2021 Jun; 103:062307. https://doi.org/10.1103/PhysRevE.103.062307 PMID: 34271687

25. Hoey GV, Clercq JD, Vanrumste B, Walle RV, Lemahieu I, Have MD, et al. EEG dipole source localization using artificial neural networks. Phys. Med. Biol. 2000 Feb; 45:997–1011. https://doi.org/10.1088/0031-9155/45/4/314 PMID: 10795987

26. Hu MK, Jing S, Du CP, Xia MY, Peng X, Guo H. Magnetic Dipole Target Signal Detection via Convolutional Neural Network. IEEE Geosci. Remote Sens. Lett. 2020 Nov; 19:1–5. https://doi.org/10.1109/LGRS.2020.3033707

27. Nicosia V, Skardal PS, Arenas A, Latora V. Collective Phenomena Emerging from the Interactions between Dynamical Processes in Multiplex Networks. Phys. Rev. Lett. 2017 Mar; 118:138302. https://doi.org/10.1103/PhysRevLett.118.138302 PMID: 28409987

28. Kumar A, Jalan S. Explosive synchronization in interlayer phase-shifted Kuramoto oscillators on multiplex networks. Chaos 2021 Apr; 31:041103. https://doi.org/10.1063/5.0043775 PMID: 34251235

29. Kumar A, Jalan S, Kachhvah AD. Interlayer adaptation-induced explosive synchronization in multiplex networks. Phys. Rev. Research 2020 Jun; 2:023259. https://doi.org/10.1103/PhysRevResearch.2.023259

30. Kachhvah AD, Dai XF, Boccaletti S, Jalan S. Interlayer Hebbian plasticity induces first-order transition in multiplex networks. New J. Phys. 2020 Dec; 22:122001. https://doi.org/10.1088/1367-2630/abcf6b

31. Rodrigues FA, Peron TKDM, Ji P, Kurths J. The Kuramoto Model in Complex Networks. Phys. Rep. 2016 Jan; 610:1–98. https://doi.org/10.1016/j.physrep.2015.10.008

32. Acebron JA, Bonilla LL, Vicente CJP, Ritort F, Spigler R. The Kuramoto model: A simple paradigm for synchronization phenomena. Rev. Mod. Phys. 2005 Apr; 77:137–185. https://doi.org/10.1103/RevModPhys.77.137

33. Kuramoto Y. Chemical Oscillations, Waves and Turbulence. London: George Alien & Unwin Ltd. Berlin, Heidelberg and New York: Springer-Verlag.; 1984. https://doi.org/10.1007/978-3-642-69689-3

34. Zou W, Zhan M, Kurths J. Phase transition to synchronization in generalized Kuramoto model with low-pass filter. Phys. Rev. E 2019 Jul; 100:012209. https://doi.org/10.1103/PhysRevE.100.012209 PMID: 31499894